Different Properties of the Native and Reconstituted Heterotrimeric G Protein Transducin[†]

Anna Goc,[‡] Thomas E. Angel,[‡] Beata Jastrzebska,[‡] Benlian Wang,[§] Patrick L. Wintrode,[||] and Krzysztof Palczewski*[,‡]

Department of Pharmacology, School of Medicine, Case Western Reserve University, Cleveland, Ohio 44106-4965, Center for Proteomics and Mass Spectrometry, School of Medicine, Case Western Reserve University, Cleveland, Ohio 44106-4988, and Department of Physiology and Biophysics, School of Medicine, Case Western Reserve University, Cleveland, Ohio 44106-4970

ABSTRACT: Visual signal transduction serves as one of the best understood G protein-coupled receptor signaling systems. Signaling is initiated when a photon strikes rhodopsin (Rho) causing a conformational change leading to productive interaction of this G protein-coupled receptor with the heterotrimeric G protein, transducin (Gt). Here we describe a new method for Gt purification from native bovine rod photoreceptor membranes without subunit dissociation caused by exposure to photoactivated rhodopsin (Rho*). Native electrophoresis followed by immunoblotting revealed that Gt purified by this method formed more stable heterotrimers and interacted more efficiently with membranes containing Rho* or its target, phosphodiesterase 6, than did Gt purified by a traditional method involving subunit dissociation and reconstitution in solution without membranes. Because these differences could result from selective extraction, we characterized the type and amount of posttranslational modifications on both purified native and reconstituted Gt preparations. Similar N-terminal acylation of the Gtα subunit was observed for both proteins as was farnesylation and methylation of the terminal Gtγ subunit Cys residue. However, hydrogen/deuterium exchange experiments revealed less incorporation of deuterium into the Gtα and Gtβ subunits of native Gt as compared to reconstituted Gt. These findings may indicate differences in conformation and heterotrimer complex formation between the two preparations or altered stability of the reconstituted Gt that assembles differently than the native protein. Therefore, Gt extracted and purified without subunit dissociation appears to be more appropriate for future studies.

The G protein transducin (Gt)[1] present in the rod outer segments (ROS) of retinal photoreceptors is a key enzyme for visual signal transduction (*1*) (reviewed in refs *2* and *3*). Gt is a heterotrimeric GTPase consisting of Gtα (~39 kDa), with a binding site for GTP or GDP (catalytic subunit), and the obligate heterodimer Gtβ (~37 kDa) and Gtγ (~6 kDa) that transfers information from photoactivated rhodopsin (Rho* or metarhodopsin II, Meta II) to its effector cGMP phosphodiesterase (cGMP PDE6) (*4*). In the dark Gt is attached to the membrane bilayer by two hydrophobic anchors (*5*). One of four different N-terminal acyl groups is connected to the Gtα amino-terminal Gly, i.e., (lauroyl (C12), myristoyl (C14), *cis*-tetradecadienoyl (C14:1) or *cis*,*cis*-tetradecadienoyl (C14:2)). Another anchor is a farnesyl (C15) group which modifies the Cys residue at the C-terminus of Gtγ (*6*−*8*).

Rho is the canonical G protein-coupled receptor (GPCR) that functions as a single photon detector (*9*−*12*). It is also one of the best studied members of a large family of cell surface receptors characterized by a typical seven-transmembrane helical topology (*13*). Recent structural studies have increased our understanding of the inactive (*13*) and photoactivated (*14, 15*) states of Rho as well as features of the apoprotein, opsin, an inactive state of Rho which displays residual Gt activity (*16*). Structural studies of GDP- (*17*) and GTP-bound (*18*) forms of Gt and other G proteins (*19*−*24*) also have enhanced our knowledge of the mechanism of Gt activation and nucleotide exchange. Three regions of Gt undergo substantial rearrangements upon GTP hydrolysis. These regions are switch I (the "effector" loop), switch II (the loop preceding the α2 helix and the helix itself), and switch III that comprises the loop connecting helix α3 to

[†] This research was supported in part by Grants EY008061, GM079191, and P30 EY11373 from the National Institutes of Health, by the Foundation Fighting Blindness, and by an unrestricted grant from Amgen Inc.

* Address correspondence to this author. Phone: 216-368-4631. Fax: 216-368-1300. E-mail: kxp65@case.edu.

[‡] Department of Pharmacology, School of Medicine, Case Western Reserve University.

[§] Center for Proteomics and Mass Spectrometry, School of Medicine, Case Western Reserve University.

[||] Department of Physiology and Biophysics, School of Medicine, Case Western Reserve University.

[1] Abbreviations: BCIP/NBT, 5-bromo-4-chloro-3-indolyl phosphate/nitroblue tetrazolium; Bis-Tris propane, 1,3-bis[tris(hydroxymethyl)methylamino]propane; cGMP, guanosine cyclic 3′,5′-monophosphate; DDM, *n*-dodecyl-β-D-maltoside; DTT, dithiothreitol; EDTA, ethylenediaminetetraacetic acid; GDP, guanosine 5′-diphosphate; GMP, guanosine 5′-monophosphate; Gt, rod photoreceptor G protein (transducin or Gt); GTPγS, guanosine 5′-3-*O*-(thio)triphosphate; GTP, guanosine 5′-triphosphate; Hepes, 4-(2-hydroxyethyl)-1-piperazinethanesulfonic acid; HPLC, high-pressure liquid chromatography; HDX, hydrogen/deuterium exchange; PDE6, rod cGMP phosphodiesterase 6; Rho, rhodopsin; Rho*, photoactivated rhodopsin; ROS, rod outer segment(s); SDS−PAGE, sodium dodecyl sulfate−polyacrylamide gel electrophoresis; TFA, trifluoroacetic acid; TPCK, L-(tosylamido-2-phenyl)ethyl chloromethyl ketone; Tricine, *N*-(2-hydroxy-1,1-bis(hydroxymethyl)-ethyl)glycine.

10.1021/bi8015444 CCC: $40.75
Published on Web 11/01/2008

strand β5 (*24*). High-resolution structures also have been determined for the complexes between G proteins and the regulator G protein signaling molecules (RGS) (*25*), G protein receptor kinase 2 (GRK2) (*26*), and phosducin (*27*) but not between G proteins and their receptors and effectors. However, analysis of existing crystal structures of Rho* (*14, 15*) and Gtiα_2/Gtsα chimeras (*18*) as well as mass spectrometric and chemical cross-linking studies have shed light on the nature of such interactions between activated GPCRs and G proteins (*28*−*31*).

Typical previous purifications of Gt have involved initial binding to Rho* and subsequent dissociation of the Gtα subunit and Gt$\beta\gamma$ from the receptor complex by addition of GTP or GTPγS. Here we describe an improved method for isolating Gt in an inactivated native state from its natural membrane source. We then compare the properties of Gt purified by our method in which Gt is extracted from dark-adapted ROS membranes (here named native Gt) with the properties of Gt isolated by a traditional method requiring dissociation of Gt by activated ROS membranes followed by its reconstitution (named reconstituted Gt). The two preparations differed both biochemically and biophysically in ways that suggest that the new preparation may be more suitable for structural studies.

MATERIALS AND METHODS

Chemicals. TPCK-treated trypsin, pepsin A, and soybean trypsin inhibitor were purchased from Worthington (Lakewood, NJ). Sequencing grade modified trypsin was purchased from Promega (Madison, WI). Sypro Ruby stain was obtained from Molecular Probes, Inc. (Paisley, UK), D_2O from Cambridge Isotope Laboratories, Inc. (Andover, MA), and DDM from Anatrace Inc. (Maumee, OH). All chemicals used for SDS−PAGE and immunoblotting were electrophoresis grade from Bio-Rad (Hercules, CA) except BCIP/NBT, which was from Promega (Madison, WI). Other chemicals were of reagent grade from Sigma (St. Louis, MO).

Antibodies and Resins. The anti-Gtα subunit (Gtα) monoclonal antibody that recognized a C-terminal epitope of Gtα (NH_2-CNLKDCGLF-OH) flanked with a N-terminal Cys residue to facilitate coupling to the carrier proteins and the anti-Rho monoclonal antibody that recognized a N-terminal epitope of Rho were generated by a conventional hybridoma technique (*32*) in our laboratory. The anti-Gtβ and the anti-Gtγ polyclonal antibodies were purchased from Santa Cruz Biotechnology Inc. (Santa Cruz, CA). Alkaline phosphatase-conjugated goat anti-mouse IgG (against Gtα) and goat anti-rabbit IgG (against Gtβ and Gtγ) from Promega were used as secondary antibodies. Protein bands were visualized with BCIP/NBT color development substrate. The propyl-agarose resin was prepared by coupling propylamine to CNBr-activated agarose (Santa Cruze Biotechnology Inc.) and 1D4 resin by coupling anti-Rho (C-terminal) monoclonal 1D4 antibody from the National Cell Culture Center (NCCC; Minneapolis, MN) to CNBr-activated Sepharose 4B according to the manufacturer's protocol. Superdex 200 10/300 GL columns were purchased from GE Healthcare Bio-Sciences (Piscataway, NJ).

Purification of Native Gt. Bovine ROS membranes were prepared from 100 frozen retinas (W. L. Lawson Co., Lincoln, NE) under dim red light according to the Paper-master procedure (*33*). To remove soluble and some membrane-associated proteins, ROS were diluted in 10 mL of isotonic buffer (20 mM Hepes, pH 7.5, 5 mM $MgCl_2$, 1 mM DTT, and 100 mM NaCl), and gently homogenized by manually passing the solution through a glass-to-glass homogenizer. The homogenized suspension was centrifuged at 25000*g* at 4 °C for 15 min, and the pellet was saved. After a second extraction, the pellet was resuspended in 10 mL of hypotonic buffer (5 mM Hepes, pH 7.5, 0.1 mM EDTA, and 1 mM DTT), the membranes were collected by centrifugation at 25000*g* at 4 °C for 45 min, and the supernatant was saved for further purification. This extraction cycle was repeated three times. All hypotonic supernatants were combined and centrifuged again at 25000*g* at 4 °C for 60 min to eliminate residual amounts of Rho-containing membranes and dialyzed overnight at 4 °C against the equilibrating buffer (10 mM Hepes, pH 7.5, 2 mM $MgCl_2$, and 1 mM DTT). This solution was applied to a 10 × 100 mm column with 3 mL of preequilibrated propyl-agarose resin at a flow rate of 15 mL/h, and then the column was washed with 3 column volumes of the equilibrating buffer. Bound proteins were eluted with a 50 mL linear gradient of 0−0.5 M NaCl in the equilibrating buffer at a flow rate of 15 mL/h, and 1 mL fractions were collected. Fractions containing Gt were pooled, dialyzed overnight at 4 °C against 10 mM Hepes, pH 7.5, containing 2 mM $MgCl_2$, 1 mM DTT, and 100 mM NaCl, and concentrated to a final volume of 0.25 mL. The sample then was injected into a Superdex 200 gel filtration column equilibrated with the buffer used for dialysis and eluted with the same buffer at a flow rate of 0.4 mL/min; 0.5 mL fractions were collected to separate PDE6 from Gt. Fractions containing Gt identified by SDS−PAGE and immunoblotting were combined and concentrated to about 2−4 mg/mL. Protein concentration was determined by the Bradford assay (*34*).

Purification of Reconstituted Gt. Preparation of bovine ROS membranes and removal of soluble proteins were performed as described above. Extraction of the membrane-associated proteins was performed according to Bigay et al. (*35, 36*). Briefly, ROS membranes washed out from soluble proteins were exposed to incandescent light for 35 min on ice and then resuspended in 10 mL of hypotonic buffer (5 mM Hepes, pH 7.5, 0.1 mM EDTA, 1 mM DTT). Next membranes were collected by centrifugation at 25000*g* at 4 °C for 45 min. This extraction was repeated three times and the supernatant discarded. Resulting membranes were suspended in hypotonic buffer supplemented with 200 μM GTP, thoroughly washed again to extract Gt, and centrifuged at 25000*g* at 4 °C for 45 min. This procedure was performed three times, and all supernatants with solubilized Gt were pooled. Finally, these extracts were cleared of ROS membrane particles by centrifugation at 25000*g* at 4 °C for 60 min, dialyzed overnight at 4 °C against equilibrating buffer (10 mM Hepes, pH 7.5, containing 2 mM $MgCl_2$ and 1 mM DTT), and loaded onto a propyl-agarose column. The next purification steps were the same as described for purification of native Gt.

Nucleotide Analyses. Nucleotides bound to Gt were identified as previously described (*37*) with a few modifications. Briefly, a sample containing 80 μg/20 μL Gt purified by either method was boiled for 3 min at 95 °C and centrifuged at 15000*g* for 20 min to remove denatured

proteins. The supernatant was collected and diluted five times with the equilibrating buffer (100 mM K_2HPO_4/KH_2PO_4, pH 6.5, containing 10 mM tetrabutylammonium bromide and 7.5% acetonitrile). An aliquot of the supernatant (100 μL) was injected into a Zorbax ODS 5 μm, 4.6 × 250 mm reverse-phase HPLC column (Agilent, Santa Clara, CA) and monitored at 254 nm. Nucleotides were eluted isocratically at a flow rate of 0.8 mL/min at ambient temperature. Nucleotides were identified by their UV spectra and elution profiles as compared with authentic GDP and GTP standards.

Limited Proteolysis of Gt. Five micrograms of native and reconstituted Gt was digested with TPCK-treated trypsin at a constant Gt:trypsin ratio of 200:1 (w/w) at 20 °C. The proteolysis was terminated at indicated times by adding an excess of the SDS−PAGE sample loading buffer and boiled for 2 min at 95 °C. All aliquots were immediately separated on 12.5% SDS−PAGE gels, and tryptic digestion products were visualized by Coomassie Blue staining.

Binding of Gt to ROS Membranes. ROS membranes stripped of soluble and membrane-associated proteins were resuspended in 20 mM Bis-Tris propane, pH 7.5, containing 1 mM $MgCl_2$, 1 mM DTT, and 120 mM NaCl at a concentration of 2 mg of Rho/mL and supplemented with 10 μg of purified native or reconstituted Gt at a constant 1:10 (w/w) Gt:Rho ratio. Samples were illuminated with a Fiber-Light covered with a 480−525 nm band-pass filter (Chroma Technology, Rockingham, VT) for 5 min or kept in the dark and then incubated 30 min at 4 °C and centrifuged at 100000*g* for 10 min. Unbound proteins present in the supernatant were quantified, whereas membranes with bound proteins were pelleted. The pellet was washed three times with 5 mM Bis-Tris propane, pH 7.5, containing 1 mM $MgCl_2$ and 1 mM DTT, and once with 20 mM Bis-Tris propane, pH 7.5, containing 1 mM $MgCl_2$, 1 mM DTT, and 120 mM NaCl. Gt protein bound to ROS membranes was extracted with 100 μM GTPγS added to 50 μL of the above buffer and analyzed by 12% Coomassie Blue stained SDS−PAGE.

Gt Activation by Rho.* Rho was purified by 1D4 affinity chromatography (*14, 38*), and activation of Gt was performed as previously described (*39, 40*). Briefly, purified native or reconstituted Gt (250 nM) was added to Rho (25 nM) in 20 mM Bis-Tris propane, pH 7.5, containing 120 mM NaCl, 5 mM $MgCl_2$, and 2 mM DDM. The sample was bleached for 15 s with a Fiber-Light covered with a 480−525 nm band-pass filter (Chroma Technology, Rockingham, VT), followed by a 10 min incubation with continuous low-speed stirring. Then 5 μM GTPγS was added, and the intrinsic fluorescence of Gtα was measured with a LS55 luminescence spectrophotometer (Perkin-Elmer, Life Science), by using excitation and emission wavelengths of 300 and 345 nm, respectively (*40*−*42*). Fluorescence change was linear within the range of protein concentrations used. No fluorescence signals were detected in the control experiment without GTPγS.

Gt Activation by Rho in a Reconstituted System.* Purified native Gt heterotrimer (40 μg) was added to 4 μg of Rho purified by 1D4 affinity chromatography or to 500 μM ROS membranes stripped of soluble and membrane-associated proteins and photoactivated for 5 min using a Fiber-Light covered with a 480−525 nm band-pass filter (Chroma Technology, Rockingham, VT), followed by a 15 min incubation on ice in the dark. Then 200 μM GTP in buffer (5 mM Hepes, pH 7.5, 0.1 mM EDTA, 1 mM DTT) was added to the samples activated by 1D4-purified Rho, and incubation in the dark was continued for the next 10 min. Then 500 μM stripped ROS membranes were added to one sample, and the other sample was left without ROS membranes. GTP (200 μM final concentration) in 5 mM Hepes, pH 7.5, containing 0.1 mM EDTA and 1 mM DTT was added to the sample activated by 500 μM Rho in stripped ROS membranes, and this sample was washed three times with hypotonic 5 mM Hepes, pH 7.5, buffer containing 0.1 mM EDTA and 1 mM DTT to extract Gt and centrifuged at 100000*g* at 4 °C for 60 min to eliminate ROS membrane particles. Next, all samples were dialyzed at 4 °C in the dark against 10 mM Hepes, pH 7.5, containing 2 mM $MgCl_2$, 1 mM DTT, and 100 mM NaCl for 24 h (*40*−*42*). Gt in the sample activated by 1D4-purified Rho and dialyzed in the presence of 500 μM stripped ROS membranes also was washed three times with the hypotonic buffer and centrifuged at 100000*g* at 4 °C for 60 min to eliminate ROS membrane particles. Then 4 μg of protein from each sample was separated in the dark by SDS−PAGE on 7.5% polyacrylamide gels under native conditions.

PDE6 Activation by Gt in a Reconstituted System. Activation of PDE6 by purified native and reconstituted Gt was carried out in the dark at room temperature. The substrate and product of PDE6, cGMP and GMP, were separated by a Zorbax ODS 5 μm, 4.6 × 250 mm reverse-phase HPLC column equilibrated with 7.5% CH_3CN/H_2O containing 10 mM tetrabutylammonium bromide and 100 mM K_2HPO_4/KH_2PO_4, pH 6.5. Nucleotides were eluted by a gradient system of 0−7.5% CH_3CN in 10 mM tetrabutylammonium bromide and 100 mM K_2HPO_4/KH_2PO_4, pH 6.5, at a flow rate of 0.8 mL/min and identified by their UV spectra and elution positions relative to authentic standards. In a typical assay, 5 nM purified PDE6 (*43*) was added to a mixture consisting of 1 μM washed ROS membranes, 0.2 μM Gt, 10 μM GTPγS, and 5 mM cGMP in 100 mM Tris, pH 7.5, containing 10 mM $MgCl_2$ and 100 mM NaCl, and the sample was immediately illuminated for 10 s. The reaction was terminated at indicated time intervals by heating the capped tube in a water bath at 95 °C for 3 min. Control experiments were performed without flash illumination and either with or without washed ROS membranes or addition of GTPγS. The resulting samples were further processed as described in the Nucleotide Analyses section.

Mass Spectroscopic Analysis of Posttranslational Modifications in Gt. Purified native and reconstituted Gt (20 μg) was dissolved in 20 μL of 100 mM Tris-HCl, pH 8.0, containing 8 M urea. Proteins then were reduced with 20 mM DTT for 2 h and treated with 50 mM iodoacetamide at 25 °C for 30 min in the dark. The alkylated proteins were diluted 10-fold in water and digested with sequencing grade modified trypsin overnight at 37 °C at a 1:50 protease:protein ratio. The resulting peptide solution was vacuum-evaporated and reconstituted in 0.1% formic acid. Proteolytic peptide analysis then was performed by using a LTQ Orbitrap XL linear ion trap mass spectrometer (Thermo Fisher Scientific, Waltham, MA) coupled with an Ultimate 3000 HPLC system (Dionex, Sunnyvale, CA). The spectra were acquired by data-dependent methods consisting of a full scan and MS/MS on the five most abundant precursor ions at the collision energy of 30%. Obtained data were submitted for a database search

using Mascot (Matrix Science, Boston, MA). To confirm the identities of modified peptides further, targeted LC-MS/MS analyses of such peptides also were done.

Hydrogen/Deuterium Exchange (HDX) Experiments. Purified native Gt was activated by 1D4-purified Rho, then supplemented with 200 μM GTP, and dialyzed in the dark at 4 °C for 24 h without ROS membranes. Purified native, reconstituted, and Rho*-activated native Gt (5 μg each) in 10 mM Hepes, pD 7.5, containing 2 mM $MgCl_2$, 1 mM DTT, 100 mM NaCl, and 95% (v/v) D_2O then was incubated at room temperature for various periods. After 0, 10, 100, or 500 s the HDX reaction was quenched by adding an equal volume of 100 mM phosphate, pH 2.5, containing 1 mM tris(2-carboxyethyl)phosphine hydrochloride, and the protein was digested on ice for 5 min with pepsin at a 1:1 (w/w) Gt:pepsin ratio. Peptic fragments were separated by reverse-phase HPLC. Control digests were initially analyzed by high-resolution tandem mass spectrometry on a FT-ICR (ThermoElectron, San Jose, CA) to allow identification of pepsin-derived parent ions, and obtained data were submitted for a database search by Mascot (Matrix Science, Boston, MA). Samples were loaded onto a Vydac TP C18 5 μm, 1 × 50 mm reverse-phase HPLC column (Grace Davison Discover Science, Deerfield, Il) for no longer than 5 min, and peptides eluted by a gradient of 2−40% acetonitrile with 0.05% TFA at a flow rate of 50 μL/min (total elution time of 13 min). Peptides separated on the column were detected on a Finnigan LTQ ion-trap mass spectrometer (ThermoElectron, San Jose, CA) directly coupled to the HPLC system by their MS/MS spectra. To slow back-exchange during this procedure, the trap and C18 columns were kept on ice. Peptide masses were calculated from the centroid of the isotopic envelope by using HD-Express software, and the extent of deuterium incorporation at each time point was determined from the shift in the mass of labeled peptides relative to their unlabeled counterparts.

Quantification of the Molar Ratio between α *and* β *Subunits in Purified Gt.* Subunits of Gt were separated by SDS−PAGE and stained with Sypro Ruby (Bio-Rad) or Coomassie Blue, and the intensity of the protein bands was quantified by Molecular Imager FX (Bio-Rad). Molar ratios between the α and β subunits in purified native and reconstituted Gt were calculated by using protein band intensity counts and the molecular masses of 39.8 kDa for Gtα and 37.4 kDa for Gtβ.

SDS−PAGE, Native PAGE, Tris/Tricine−PAGE, and Immunoblotting. Protein separation was performed on 12% SDS−PAGE or 16.5% Tris/Tricine polyacrylamide gels. We used 7.5% polyacrylamide gels to test whether α, β, and γ subunits of native and reconstituted Gt formed a stable complex after purification. Coomassie Blue R250 staining and immunoblotting (Immobilon-P PVDF; Millipore) were done according to standard protocols.

RESULTS

Purification of Gt. Gt was isolated by two methods for this work. The newly developed technique is a variation of the isolation procedure described by Baehr and Applebury (*44*). We refer to this isolation as purification of native Gt (Figure S1 of Supporting Information) because the procedure was done under dim red light to prevent Rho → Rho* transformation and consequent Gt binding to Rho*, activation, and subunit dissociation. The second traditional isolation was performed according to the method developed by Bigay and Chabre (*35, 36*). This isolation is referred to as purification of reconstituted Gt (Figure S2 of the Supporting Information) because it involves reconstitution in solution of Gtα and Gt$\beta\gamma$ after they have dissociated from Rho*. Both procedures involved washing ROS membranes in isotonic buffer to remove most of the soluble and some membrane-associated proteins. After washing out soluble protein in isotonic buffer (Figure S1a, lanes I of the Supporting Information), Gt was efficiently extracted in hypotonic buffer without bleaching Rho in ROS membranes and addition of GTP (Figure S1a, lanes H of the Supporting Information). Next, the Gt extract was purified on an alkyl-agarose column. We had tested several different resins for purification of Gt, i.e., hexyl-agarose, hydroxyapatite, pentyl-agarose, and butyl-agarose resins, all in combination with gel filtration chromatography. The best results in terms of yield and purity were achieved with a propyl-agarose resin (Figure S1b of the Supporting Information). Fractions primarily containing Gt were pooled, concentrated, and then purified by gel filtration chromatography using a Superdex 200 column (Figure S1c of the Supporting Information). In the second (traditional) method, following bleaching of Rho in ROS membranes, PDE6 was first extracted along with remaining peripheral proteins, and then Gt was extracted with 200 μM GTP in hypotonic buffer (Figure S2a of the Supporting Information). Fractions containing Gt from the propyl-agarose column (Figure S2b of the Supporting Information) were pooled, concentrated, and finally purified on a Superdex 200 column (Figure S2c of the Supporting Information). Because it was reported that ROS contain an excess of Gt$\beta\gamma$ over Gtα (*45*), the ratio between the α and β subunits in purified Gt was quantified as described in Materials and Methods (Figures S1d and S2d of the Supporting Information). This ratio was determined to be one molecule of Gtα per one molecule of Gtβ for both purification procedures. Gt was purified to apparent homogeneity by both purification methods, yielding 2−4 mg of purified protein from 100 bovine retinas.

Biochemical Characterization of Gt. Native and reconstituted Gt were analyzed by SDS−PAGE, Tris/Tricine−PAGE and native PAGE (Figure 1). Proteins from both preparations were separated on 12% SDS−PAGE, and the resolved bands were identified by immunoblotting with antibodies against the Gtα and Gtβ subunits. The Gtγ subunit was visualized on a 16.5% polyacrylamide Tris/Tricine gel, and its identity was confirmed by immunoblotting (Figure 1a). Native electrophoresis followed by immunoblotting was performed to assess the stability of the heterotrimer complexes formed by native and reconstituted Gt. The heterotrimer of native Gt migrated as a single band in native gels, whereas the reconstituted protein dissociated into subunits (Figure 1b), indicating lower stability of the latter complex.

Similar to reconstituted Gt, native Gt, once activated by either 1D4-purified Rho* or Rho* in native ROS membranes and then reconstituted overnight by dialysis with or without ROS membranes, migrated as separate bands on native PAGE (Figure S3 of the Supporting Information). Thus, activation of Gt causes separation of the subunits that cannot be fully reversed by reconstitution with the conventional

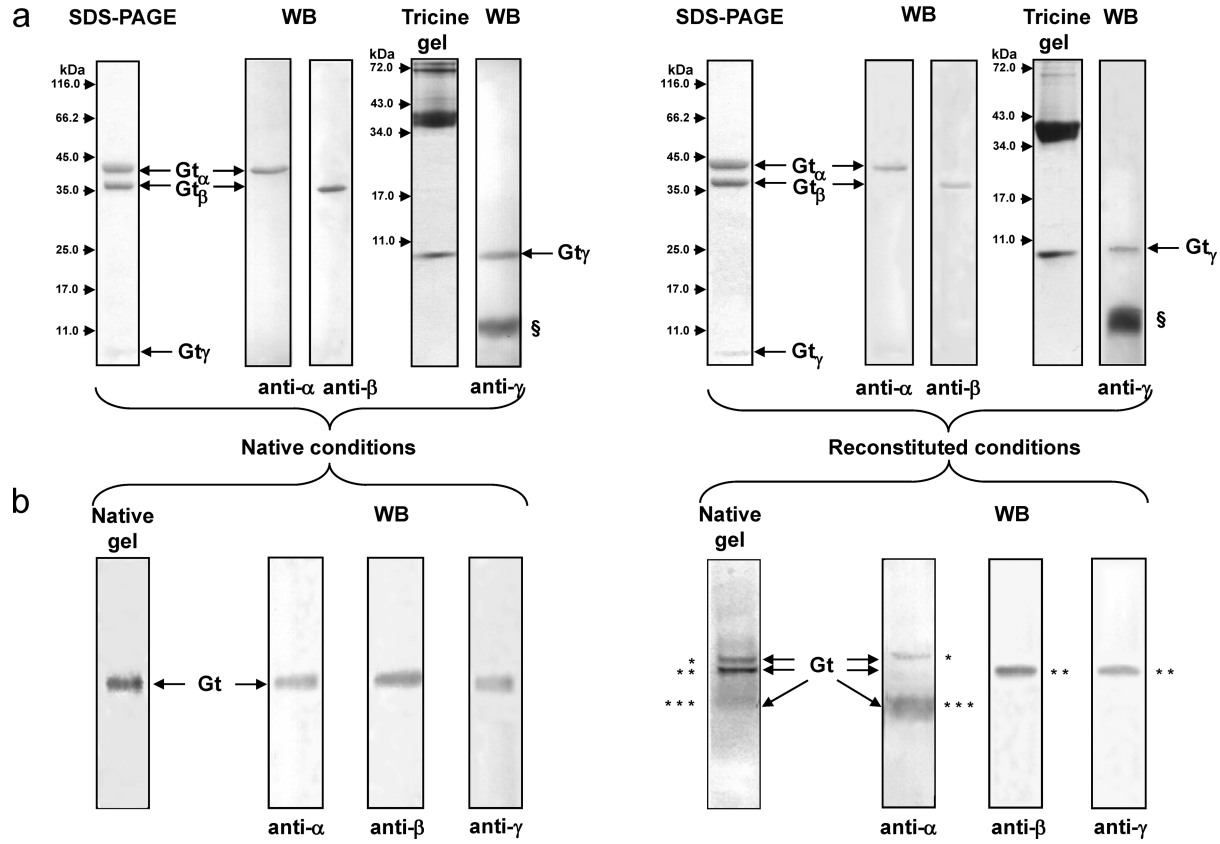

FIGURE 1: Electrophoretic characterization of purified native and reconstituted Gt. (a) Separation of native Gt and reconstituted Gt after gel filtration on 12% SDS−PAGE gels (2 μg) and on a 16.5% Tris/Tricine polyacrylamide gel (5 μg). The Gt α, β, and γ subunits present in these protein preparations were confirmed by immunoblotting (WB) analysis. (b) Native electrophoresis of 2 μg of Gt on 7.5% polyarylamide gels and confirmation of the subunits present in separated bands by immunoblotting (WB). Key: §, front of dye from sample loading buffer; *, Gtα; **, Gt$\beta\gamma$; ***, Gtα.

dialysis procedure (Figure 3 III of the Supporting Information) or by addition of diluted ROS membranes (Figure S3 IV and V of the Supporting Information) even though the nucleotide content in both native and reconstituted Gt was found to be similar (Figure 4 of the Supporting Information).

These differences in behavior during native electrophoresis prompted us to characterize both native and reconstituted Gt in more detail. We subjected both purified preparations to enzymatic digestion with TPCK-trypsin at a protease to substrate ratio of 1:200 (w/w). The reaction was terminated by adding an excess of the SDS−PAGE loading buffer, and polypeptides in the digest were immediately separated on 12.5% SDS gels. After incubating the samples for 30 min or more, it became evident that the proteolysis of reconstituted Gt proceeded faster, indicating greater accessibility of cleavage sites and, therefore, lesser stability (Figure S5 of the Supporting Information).

To determine if such differences in stable complex formation and limited proteolysis might correlate with Gt activation, we measured the rate of Gt activation by monitoring the changes in intrinsic Trp fluorescence emission of the Gtα subunit in response to binding GTPγS (*38, 39*). Although a Trp fluorescence increase was observed for both Gt preparations, the rate of native Gt activation was 1.5 times that of reconstituted Gt (Figure 2a). Next, when Gt binding to ROS membranes was examined by SDS−PAGE (Figure 2b, left and middle panels), this analysis showed less efficient binding of reconstituted Gt, as judged from the intensities of unbound fractions. Band intensity quantification showed that 30% less of the Gtα subunit and 18% less of the Gtβ subunit of reconstituted Gt were bound to ROS as compared to the corresponding subunits of native Gt (Figure 2b, right panel).

We also examined whether PDE6 could be activated by Gt. PDE6 is a heterotetrameric enzyme composed of α, β, and γ subunits, with a ratio 1:1:2 that rapidly hydrolyzes cGMP to GMP when stimulated by Gtα-GTP subunits (*45*). Our data showed that PDE6 activated by reconstituted Gt had only 25% the activity of PDE6 activated by native Gt (Figure 3).

Posttranslational Modifications of Gt. Biochemical differences between native and reconstituted Gt then led us to characterize the posttranslational lipid modifications at the N-terminus of Gtα and C-terminus of Gtγ of both purified Gt preparations. Fukada et al. first observed a Gt-linked fatty acid distribution composed of lauroyl (C12:0), *cis*,*cis*-tetradecadienoyl (C14:2), *cis*-tetradecadienoyl (C14:1), and myristoyl (C14:0) groups on the Gtα subunit (*6*). Additionally, the Gtγ subunit C-terminal Cys was shown to be farnesylated and farnesyl-methylated (*7*). As shown in Figure 4a, our results agree with previous reports with one exception; i.e., we did not observe a myristoyl modification of the α subunit of Gt in protein obtained by either purification procedure. A relative quantification of Gtα subunit N-terminal lipid modifications was derived from the intensity ratios of parental ions for each modified peptide species. Heterogeneity of lipid modification was found with the most abundant modification consisting of C14:2 followed by C14:1

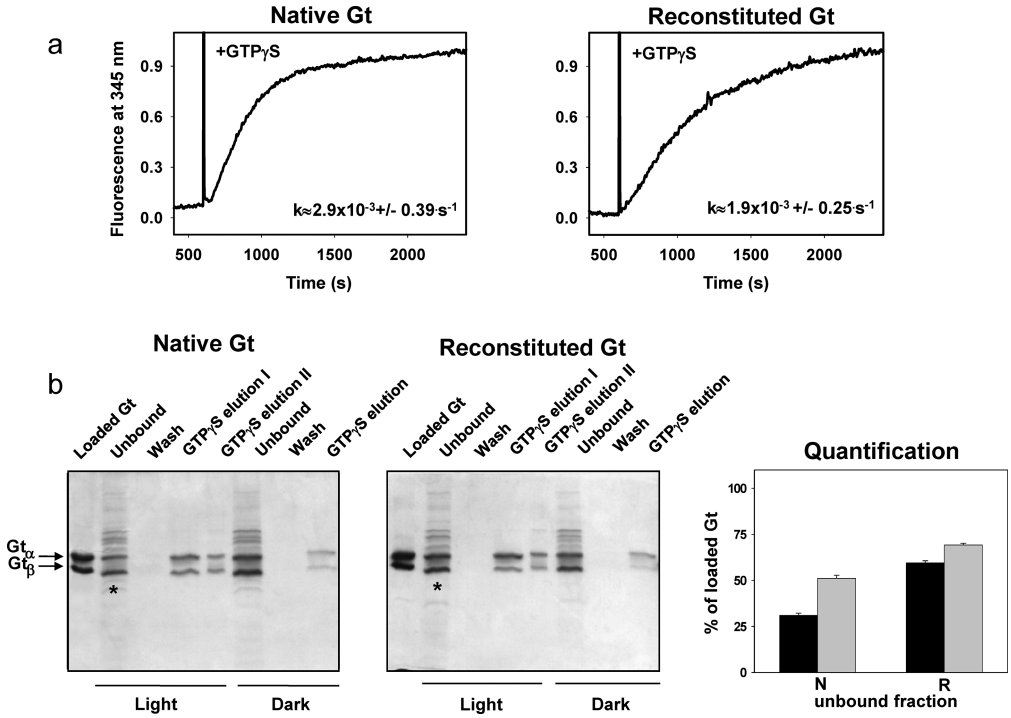

FIGURE 2: Binding of Gt to ROS membranes and its activity. (a) Intrinsic fluorescence increase of the Gtα subunit due to interaction with photoactivated 1D4-purified Rho. The reaction was carried out at 20 °C in a continuously stirred cuvette with 25 nM Rho and 250 nM Gt in 10 mM Bis-Tris propane, 120 mM NaCl, 5 mM $MgCl_2$, and 2 mM DDM (pH 7.5). 5 μM GTPγS was added after 600 s of recording. Relative activation rates (k) were calculated from three independent experiments. (b) Native Gt and reconstituted Gt were mixed with stripped ROS membranes at a 1:10 (w/w) Gt:Rho ratio and illuminated or incubated in the dark as described in Materials and Methods. Then bound Gt was extracted from ROS membranes after addition of 100 μM GTPγS. Proteins bound to ROS membranes were analyzed by 12% Coomassie Blue stained SDS−PAGE (respectively left and middle panels). *: Quantification of unbound Gtα and Gtβ subunits extracted from bleached and unbleached ROS membranes and purified by adsorption on a propyl-agarose resin followed gel filtration of the eluted samples was performed as described in Materials and Methods (data shown in the right lower panel). Key: (black) Gtα; (gray) Gtβ; N, native Gt; R, reconstituted Gt.

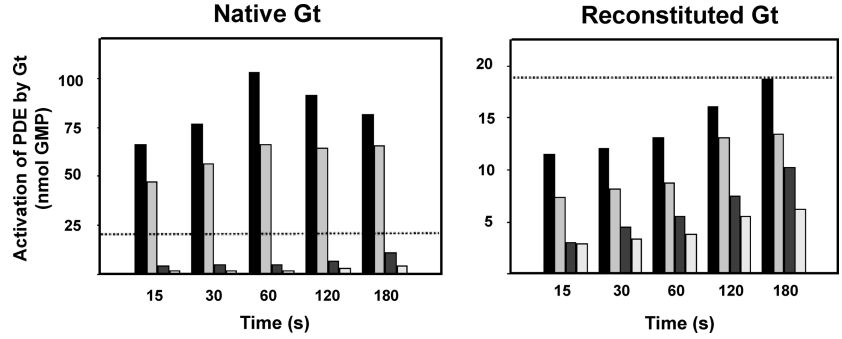

FIGURE 3: Activated PDE6 as a substrate for Gt. Time course of cGMP hydrolysis by PDE6 in the presence of activated Gt and stripped bovine ROS membranes assessed by reverse-phase HPLC separation of GMP. All experiments were performed in the dark either with (black, sample) or without (gray, controls) flash illumination at 20 °C of mixtures containing membranous Rho (1 μM), native or reconstituted Gt (0.2 μM), GTPγS (10 μM), and cGMP (5 mM). In both cases the reaction was started at time 0 by addition of 5 nM PDE6 purified by propyl-agarose resin and subsequent gel filtration chromatography. (black) PDE6, Gt, ROS, cGMP, and GTPγS, light; (light gray) PDE6, Gt, ROS, cGMP, and GTPγS, no light; (dark gray) PDE6, ROS, and cGMP, no light; (white) PDE6, Gt, cGMP, and GTPγS, no light. The horizontal dotted line displays the maximum activity of reconstituted transducin.

and C12:0 being the least abundant. Gtγ subunit carboxyl terminus modifications also were detected with an abundance of C15 > C15-Met (Figure 4b). These results demonstrate that both preparations (native and reconstituted) had similar posttranslational modifications on both subunits of Gt. Thus, the distinct biochemical properties of each Gt preparation cannot be explained by selective extraction of differently modified protein subspecies.

HDX Experiments. We performed HDX experiments to assess the nature of the structural differences between native and reconstituted Gt. Native Gt, reconstituted Gt, and, as a control, native Gt activated by 1D4-purified Rho were supplemented by 200 μM GTP and dialyzed overnight; each was incubated with D_2O-containing buffer for 10, 100, and 500 s to follow HDX. After reduction of the disulfide bond with tris(2-carboxyethyl)phosphine hydrochloride and digestion with pepsin, samples were subjected to rapid HPLC mass spectroscopic analyses. Overall peptide coverage of the primary sequence was 17% for Gtα and 49% for Gtβ that fortunately included the critical switch regions. Similar levels of deuterium incorporation were observed for reconstituted Gt and Gt activated by Rho* (panels a and b of Figure 5),

a

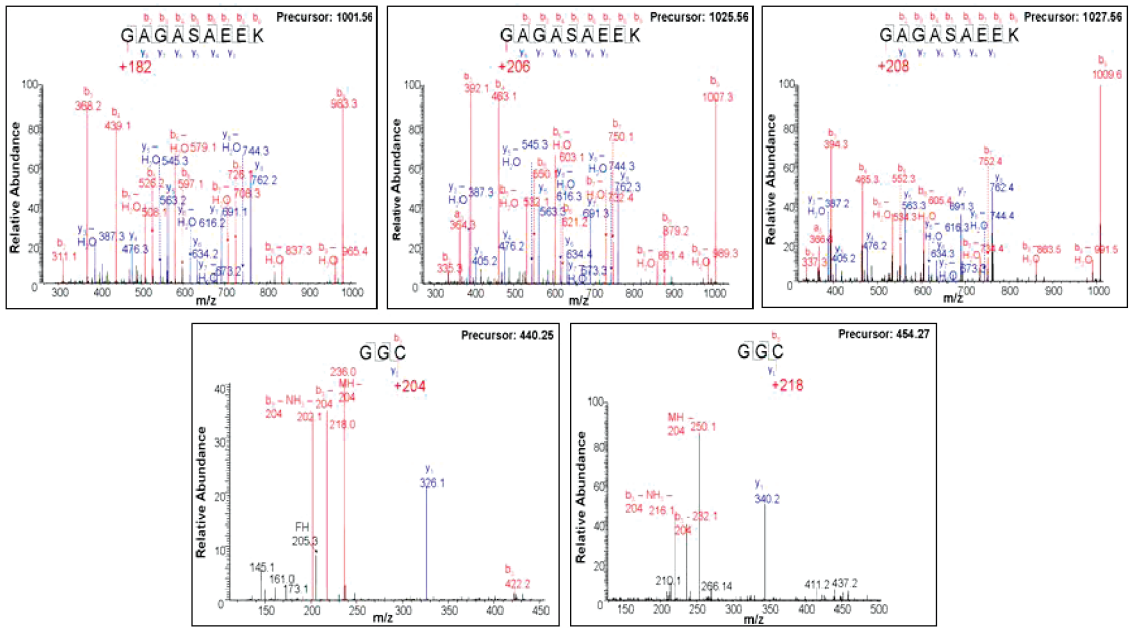

b

Type of Gt subunit	Observed polypeptide	Mass of observed and modified peptides	Type of modification	Ratio					
				N	R	N	R	N	R
alpha	GAGASAEEK	1001.56	C12	C14:2/C12		C14:1/C12		C14:2/C14:1	
	GAGASAEEK	1025.56	C14:2						
	GAGASAEEK	1027.56	C14:1	**5.0**	2.5	**2.0**	1.5	**2.3**	1.8
gamma	GGC	440.25	C18	C15/C15-Met					
	GGC	454.27	C18-Met	**9.5**	7.0				

FIGURE 4: Posttranslational modification of Gt. (a) Tandem mass spectra of the modified peptides of Gt purified under dark conditions: GAGASAEEK, N-terminal of the Gtα subunit; GGC, C-terminal of the Gtγ subunit. (b) Mass spectroscopic characterization of modified peptides in Gt. The analysis was carried out as described in Materials and Methods.

indicating similar structural dynamics for the proteins in these two samples. These two preparations also incorporated more deuterium than native Gt. For example, peptides ^{156}ERLVTPGYVPTEQDVL^{171} and ^{186}SFKDLNF^{192} of the Gtα subunit showed an increased level of deuterium incorporation in both reconstituted Gt and activated Gt relative to native Gt. Importantly, the detected peptide ^{186}SFKDLNF^{192} (Figure 5a) represents a part of the switch I region on the Gtα subunit that is linked to stable heterotrimeric complex formation; others have shown that this peptide is drawn toward the nucleotide-binding pocket upon nucleotide exchange (*17, 33*). We also observed increased levels of HDX in some regions of the Gtβ subunit. Peptides ^{70}LVSASQDKL^{79}, ^{191}SLAPDTRL^{198}, ^{199}FVSGACDASKL^{210}, ^{253}FDLRADQEL^{261}, and ^{309}AGHDNRVSCL^{318} all manifested an increase in deuterium uptake in samples of both reconstituted Gt and activated Gt relative to native Gt. Significantly, peptide ^{70}LVSASQDKL^{79} of the Gtβ subunit, found at the interface between the β subunit and the functionally important switch I region of the α subunit, displayed increased deuterium uptake in reconstituted Gt and activated Gt. The mass spectrum of peptide ^{309}AGHDNRVSCL^{318} of the β subunit that interacts with the switch II region of the α subunit (*46, 47*) also showed more deuterium uptake when derived from reconstituted Gt as compared to native Gt (Figure 5b). These measurements were performed several times ($n \geq 3$) with similar results. Many other peptides showed no change in HDX in the reconstituted sample, indicating that the exchange reflects real structural differences rather than a systematic error.

DISCUSSION

Recent progress in elucidating the structures of GPCRs and their interacting partners has focused more attention upon the signaling GPCR-G protein complex. In this study we examined the heterotrimeric G protein of the visual signal transduction cascade, transducin (Gt), that has been extensively characterized in recent years (*48*). Based on the idea that limited success in generating the Rho*-Gt complex might reflect an altered structure of Gt, we purified native Gt by a different method so that it might exhibit all of its expected properties. Here we present evidence that the complex of heterotrimeric subunits of Gt can be altered depending on the purification procedure. Moreover, the new method yielded nearly homogeneous Gt with superior functional characteristics compared to purified Gt reconstituted from its subunits.

Purification of Gt. We extracted native Gt by using an approach based on the method of Baehr and Applebury (*44*). Modifications of their procedure resulted in a scalable and highly reproducible means of obtaining highly active Gt. This simple and rapid method relied on isolation of ROS, compartments of retinal rod cells that are highly enriched in Gt and contain all of the components required for phototransduction. Gt was extracted from ROS membranes by washes with appropriate ionic strength buffers and then purified by adsorption to a weakly hydrophobic propyl-agarose resin.

The use of propyl-agarose was especially beneficial because the eluted Gt was more concentrated than that eluted

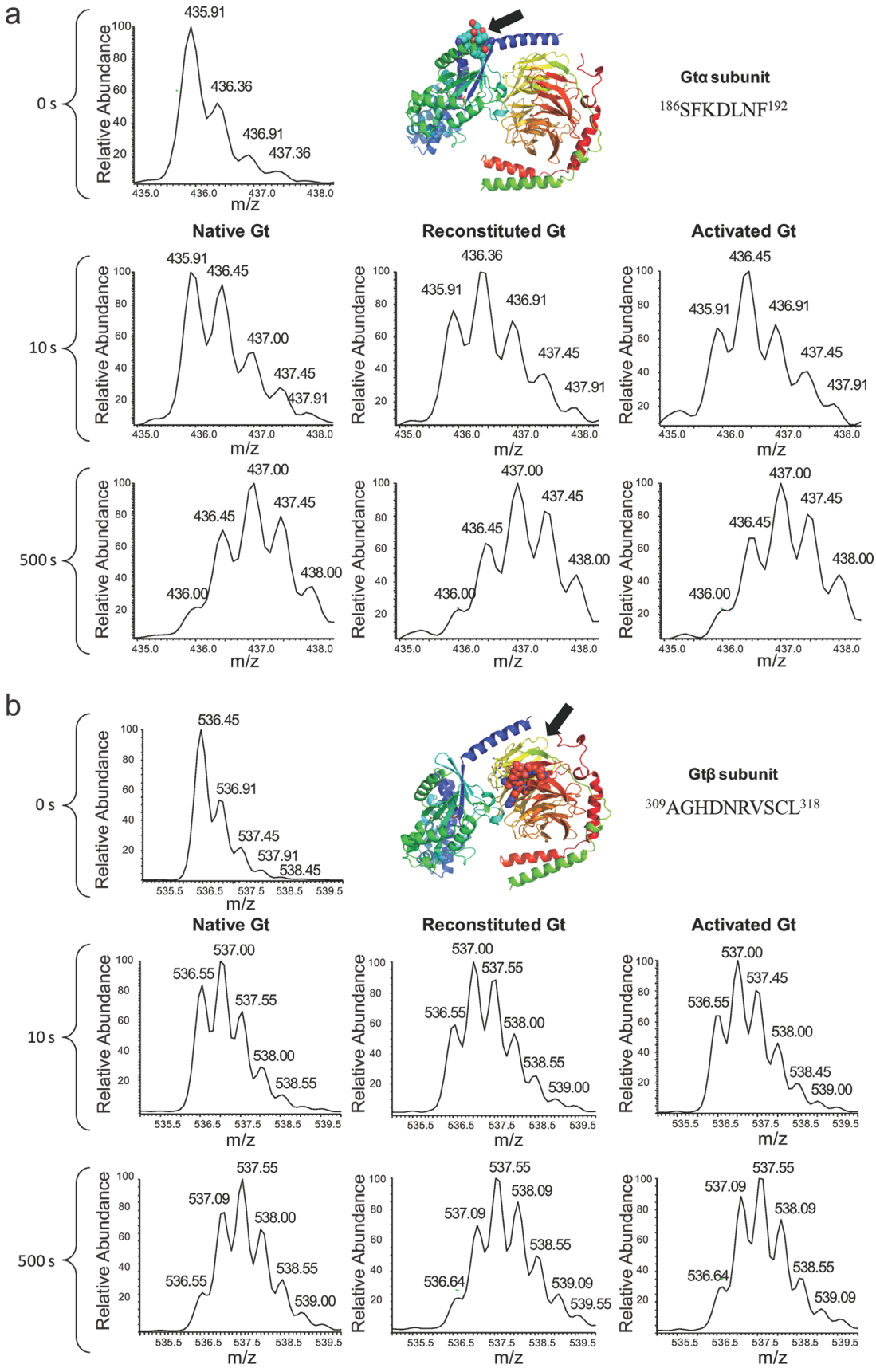

FIGURE 5: Deuterium incorporation by Gt peptides. Reconstituted Gt exhibited more deuterium incorporation than native Gt extracted under dim red light. (a) Peptide ^{186}SFKDLNF^{192} on the Gtα subunit incorporated more deuterium following a 10 s incubation in deuterated solvent with reconstituted Gt as compared to native Gt (left and center panels). (b) Differential deuterium incorporation also was observed for the Gtβ subunit on peptide ^{309}AGHDNRVSCL^{318} located at the interface between the Gtα and Gtβ subunits (left and center panels). Native Gt activated by purified Rho* exhibited a similar pattern of deuterium incorporation as reconstituted Gt for all peptides detected (right panels in parts a and b).

from hexyl-agarose or other resins (*43, 49*). Except for PDE, few other proteins were retained on the propyl-agarose resin. The subsequent gel filtration step separated Gt from PDE. The Gtα and Gtβ subunits displayed the proper 1:1 subunit stoichiometry.

Then we compared the above purified preparation of native unactivated Gt with reconstituted Gt purified by the method used by Bigay and Chabre (*35, 36*). The latter procedure requires initial coupling of Gt with Rho* in the absence of nucleotide. After ROS membranes are illuminated, both soluble proteins and proteins loosely associated with membranes are removed by repetitive washes. Gt in the form of its subunits, Gtα-GTP and Gt$\beta\gamma$, is released from the membrane-associated receptor complex after addition of GTP. The Gtα-GTP and Gt$\beta\gamma$ subunits then are isolated. The last phase of this heterotrimeric G protein extraction relies on the intrinsic GTPase activity of Gt wherein the Gtα-GTP subunit is converted first to a Gtα-GDP complex that then reassociates with the Gt$\beta\gamma$ subunits. This method has been used extensively in recent work to purify Gt or its mutants (*50*−*52*), to produce isotopically labeled Gt (*53, 54*), and to reassemble modified subunits of Gtα-GTP into functional heterotrimetic Gt-GDP (*55*). Similarly, other G proteins have been reassembled from Gtα-GDP and Gt$\beta\gamma$ subunits (*26*).

Characterization of Native and Reconstituted Gt. Analysis of purified Gt by native electrophoresis revealed striking nonhomogenous behavior of reconstituted Gt. Two species of different mobility were identified compared to native Gt purified under darkened conditions where only one band consisting of α, β, and γ subunits of Gt was found. This result strongly indicates that assembly of Gt subunits differs between the two purified preparations. Furthermore, reconstituted Gt showed a relative decrease in the rates of nucleotide exchange and PDE activation, both indicative of functional deficiencies in the heterotrimeric complex. These inadequacies did not result from aberrant nucleotide content because reconstituted Gt contained GDP, indicating that GTP had been appropriately hydrolyzed to GDP in the reconstituted Gt isolates. Membrane binding was assessed to determine if the observed differences in activity were due to a deficiency in membrane binding and/or receptor association. The observed coupling efficiency was lower for reconstituted Gt than for native Gt. This result might suggest that some fraction of Gt could not be properly reconstituted due to permanent changes in subunit reassembly. Treatment of both forms of Gt with trypsin exhibited subtle differences in proteolysis patterns between them. Our analysis of digestion patterns concluded, in agreement with Fung and Nash (*55*), that a conformational transition of the Gtα subunit occurs upon conversion of GDP to GTP and does not recover after GTP hydrolyzes to GDP, suggesting structural differences in protein isolates following the interaction with Rho*. These differences cannot be attributed to differences in posttranslational modifications as evidenced by a similar subset of these modifications in both Gt preparations.

Binding of native and reconstituted Gt to ROS membranes also differed. Our results indicate that the photoactivation cycle with Rho* weakens the interaction of both the Gtα and Gt$\beta\gamma$ subunits in this heterotrimer and also suggests the existence of some amount of "leaky" Gt$\beta\gamma$ dimer. We encountered the same phenomenon when trying to purify the Rho*-Gt complex by other techniques such as gel filtration or concanavalin A affinity chromatography (data not shown). So there are at least two possible explanations for the above observations: one is that during purification we obtained Gt enriched by an excess of Gt$\beta\gamma$ dimers that could not rebind to ROS membranes. Others have shown that ROS membranes contain about three to four times more $\beta\gamma$ dimers than α subunits (*44*). But we used Gt proteins with quantified 1:1 ratios of Gtα to Gtβ. Second, it is also possible that there is constant exchange between Rho-bound and free Gt during cellular signaling transitions. While the Gtα subunit stays tightly bound to Rho*, the Gt$\beta\gamma$ dimer may need to be exchanged. This hypothesis would explain the need for a higher abundance of Gt$\beta\gamma$ dimer in ROS membranes.

HDX of Native and Reconstituted Gt. Several differences noted between deuterium incorporation in the Gtα (Figure 5a) and Gtβ (Figure 5b) subunits of both proteins provide important insights into structural differences between reconstituted and native Gt. Increased deuterium incorporation detected at early time points in reconstituted Gt relative to native Gt probably indicates an increase in intra- and intermolecular interactions in the reconstituted protein. Increased deuterium incorporation into peptides of the switch I region of reconstituted Gt compared to native Gt, specifically into peptide ^{186}SFKDLNF^{192} containing the carboxyl-terminal residues of the switch I region known to be important for nucleotide exchange, is consistent with the results of the Gt activation assay (Figure 2a) showing slower activation for reconstituted Gt. Additionally, the SDS−PAGE data demonstrating reduced binding of the Gtα subunit to ROS membranes are consistent with the HDX experiments (Figure 2b) showing greater perturbations in peptide ^{186}SFKDLNF^{192} as this peptide is adjacent to the carboxyl-terminal domain of the Gtα subunit that participates in receptor binding (*56*). Differences in intra- and intermolecular interactions at the switch II region of Gtα and the adjacent region of Gtβ subunits also are indicated by the HDX studies. Results of the HDX studies also support the observed functional differences between native and reconstituted Gt in the PDE6 activation assay (Figure 3), as the switch II region is involved in effector PDE6 coupling. Differences in stable heterotrimeric complex formation observed by PAGE analysis (Figure 1b) are consistent with the observed reduction in intermolecular interactions indicated by HDX results for the reconstituted Gt as well. Peptides ^{199}FVSGACDASKL^{210} and ^{253}FDLRADQEL^{261} in the Gtβ subunit (both located at the interface between the Gtβ subunit and the Gtγ subunit) exhibited increased deuterium uptake indicating differences in the heterodimer complex in reconstituted Gt as compared to native Gt preparations. The difference in Gt$\beta\gamma$ subunit interaction manifested by increased HDX in reconstituted Gt is consistent with the decreased activation revealed by the Gt activation (Figure 2a) and Rho binding assays (Figure 2b) given that the carboxyl-terminal sequence in the Gtγ subunit has been shown to interact with and stabilize Meta II (*57, 58*).

CONCLUSIONS

Our study highlights the importance of native assembly for Gt. After purification, both proteins were active but native

Gt extracted directly from ROS under dim red light displayed higher activity in interacting with both Rho*-containing membranes and PDE. Regions of the heterotrimeric G protein associated with function showed structural differences in our HDX experiments that are consistent with differences observed at the biochemical level. Thus, HDX experiments alone showed unequivocal structural differences between native and reconstituted Gt. This observation could limit methodologies used to study its interaction of Gt with membrane-bound Rho*.

ACKNOWLEDGMENT

We thank Dr. Marcin Golczak (Case Western Reserve University) for help during the course of this study and Dr. Leslie T. Webster, Jr., and members of the Palczewski laboratory (Case Western Reserve University) for valuable comments on the manuscript.

SUPPORTING INFORMATION AVAILABLE

Two-step purification of native Gt (Figure 1S), two-step purification of reconstituted Gt (Figure 2S), native Gt activation by Rho* (Figure 3S), nucleotide analyses of Gt (Figure 4S), and limited proteolysis of native and reconstituted Gt (Figure 5S). This material is available free of charge via the Internet at http://pubs.acs.org.

REFERENCES

1. Fung, B. K., and Stryer, L. (1980) Photolyzed rhodopsin catalyzes the exchange of GTP for bound GDP in retinal rod outer segments. *Proc. Natl. Acad. Sci. U.S.A. 77*, 2500–2504.
2. Arshavsky, V. Y., Lamb, T. D., and Pugh, E. N., Jr. (2002) G proteins and phototransduction. *Annu. Rev. Physiol. 64*, 153–187.
3. Polans, A., Baehr, W., and Palczewski, K. (1996) Turned on by Ca^{2+}! The physiology and pathology of Ca^{2+}-binding proteins in the retina. *Trends Neurosci. 19*, 547–554.
4. Hamm, H. E. (1998) The many faces of G protein signaling. *J. Biol. Chem. 273*, 669–672.
5. Zhang, Z., Melia, T. J., He, F., Yuan, C., McGough, A., Schmid, M. F., and Wensel, T. G. (2004) How a G protein binds a membrane. *J. Biol. Chem. 279*, 33937–33945.
6. Kokame, K., Fukada, Y., Yoshizawa, T., Takao, T., and Shimonishi, Y. (1992) Lipid modification at the N terminus of photoreceptor G-protein alpha-subunit. *Nature 359*, 749–752.
7. Fukada, Y., Takao, T., Ohguro, H., Yoshizawa, T., Akino, T., and Shimonishi, Y. (1990) Farnesylated gamma-subunit of photoreceptor G protein indispensable for GTP-binding. *Nature 346*, 658–660.
8. Lai, R. K., Perez-Sala, D., Canada, F. J., and Rando, R. R. (1990) The gamma subunit of transducin is farnesylated. *Proc. Natl. Acad. Sci. U.S.A. 87*, 7673–7677.
9. Filipek, S., Stenkamp, R. E., Teller, D. C., and Palczewski, K. (2003) G protein-coupled receptor rhodopsin: A prospectus. *Annu. Rev. Physiol. 65*, 851–879.
10. Palczewski, K. (2006) G protein-coupled receptor rhodopsin. *Annu. Rev. Biochem. 75*, 743–767.
11. Ridge, K. D., Abdulaev, N. G., Sousa, M., and Palczewski, K. (2003) Phototransduction: crystal clear. *Trends Biochem. Sci. 28*, 479–487.
12. Ridge, K. D., and Palczewski, K. (2007) Visual rhodopsin sees the light: structure and mechanism of G protein signaling. *J. Biol. Chem. 282*, 9297–9301.
13. Palczewski, K., Kumasaka, T., Hori, T., Behnke, C. A., Motoshima, H., Fox, B. A., Le Trong, I., Teller, D. C., Okada, T., Stenkamp, R. E., Yamamoto, M., and Miyano, M. (2000) Crystal structure of rhodopsin: A G protein-coupled receptor. *Science 289*, 739–745.
14. Salom, D., Lodowski, D. T., Stenkamp, R. E., Le Trong, I., Golczak, M., Jastrzebska, B., Harris, T., Ballesteros, J. A., and Palczewski, K. (2006) Crystal structure of a photoactivated deprotonated intermediate of rhodopsin. *Proc. Natl. Acad. Sci. U.S.A. 103*, 16123–16128.
15. Salom, D., Le Trong, I., Pohl, E., Ballesteros, J. A., Stenkamp, R. E., Palczewski, K., and Lodowski, D. T. (2006) Improvements in G protein-coupled receptor purification yield light stable rhodopsin crystals. *J. Struct. Biol. 156*, 497–504.
16. Park, J. H., Scheerer, P., Hofmann, K. P., Choe, H. W., and Ernst, O. P. (2008) Crystal structure of the ligand-free G-protein-coupled receptor opsin. *Nature* (in press).
17. Noel, J. P., Hamm, H. E., and Sigler, P. B. (1993) The 2.2 Å crystal structure of transducin-alpha complexed with GTP gamma S. *Nature 366*, 654–663.
18. Lambright, D. G., Noel, J. P., Hamm, H. E., and Sigler, P. B. (1994) Structural determinants for activation of the a-subunit of a heterotrimeric G protein. *Nature 369*, 621–628.
19. Tesmer, J. J., Sunahara, R. K., Gilman, A. G., and Sprang, S. R. (1997) Crystal structure of the catalytic domains of adenylyl cyclase in a complex with GsaGTPgS. *Science 278*, 1907–1916.
20. Coleman, D. E., Berghuis, A. M., Lee, E., Linder, M. E., Gilman, A. G., and Sprang, S. R. (1994) Structures of active conformations of Gia_1 and the mechanism of GTP hydrolysis. *Science 265*, 1405–1412.
21. Kleuss, C., Raw, A. S., Lee, E., Sprang, S. R., and Gilman, A. G. (1994) Mechanism of GTP hydrolysis by G-protein a subunits. *Proc. Natl. Acad. Sci. U.S.A. 91*, 9828–9831.
22. Wall, M. A., Coleman, D. E., Lee, E., Iniguez-Lluhi, J. A., Posner, B. A., Gilman, A. G., and Sprang, S. R. (1995) The structure of the G protein heterotrimer $Gia_1b_1g_2$. *Cell 83*, 1047–1058.
23. Coleman, D. E., and Sprang, S. R. (1999) Structure of Gia_1·GppNHp, autoinhibition in a Ga protein-substrate complex. *J. Biol. Chem. 274*, 16669–16672.
24. Sprang, S. R. (1997) G protein mechanisms: insights from structural analysis. *Annu. Rev. Biochem. 66*, 639–678.
25. Slep, K. C., Kercher, M. A., He, W., Cowan, C. W., Wensel, T. G., and Sigler, P. B. (2001) Structural determinants for regulation of phosphodiesterase by a G protein at 2.0 Å. *Nature 409*, 1071–1077.
26. Tesmer, V. M., Kawano, T., Shankaranarayanan, A., Kozasa, T., and Tesmer, J. J. (2005) Snapshot of activated G proteins at the membrane: the Galphaq-GRK2-Gbetagamma complex. *Science 310*, 1686–1690.
27. Gaudet, R., Savage, J. R., McLaughlin, J. N., Willardson, B. M., and Sigler, P. B. (1999) A molecular mechanism for the phosphorylation-dependent regulation of heterotrimeric G proteins by phosducin. *Mol. Cell 3*, 649–660.
28. Angel, T. E., Kraft, P. C., and Dratz, E. A. (2006) Metarhodopsin-II stabilization by crosslinked Gtalpha C-terminal peptides and implications for the mechanism of GPCR-G protein coupling. *Vision Res. 46*, 4547–4555.
29. Janz, J. M., and Farrens, D. L. (2003) Assessing structural elements that influence Schiff base stability: mutants E113Q and D190N destabilize rhodopsin through different mechanisms. *Vision Res. 43*, 2991–3002.
30. Wang, X., Kim, S. H., Ablonczy, Z., Crouch, R. K., and Knapp, D. R. (2004) Probing rhodopsin-transducin interactions by surface modification and mass spectrometry. *Biochemistry 43*, 11153–11162.
31. Filipek, S., Krzysko, K. A., Fotiadis, D., Liang, Y., Saperstein, D. A., Engel, A., and Palczewski, K. (2004) A concept for G protein activation by G protein-coupled receptor dimers: the transducin/rhodopsin interface. *Photochem. Photobiol. Sci. 3*, 628–638.
32. Campbell, A. M. (1984) *Monoclonal antibody technology: the production and characterization of rodent and human hybridomas*, Elsevier, Amsterdam and New York.
33. Papermaster, D. S. (1982) Preparation of retinal rod outer segments. *Methods Enzymol. 81*, 48–52.
34. Bradford, M. M. (1976) A rapid and sensitive method for the quantitation of microgram quantities of protein utilizing the principle of protein-dye binding. *Anal. Biochem. 72*, 248–254.
35. Bigay, J., and Chabre, M. (1994) Purification of transducin. *Methods Enzymol. 237*, 139–146.
36. Bigay, J., and Chabre, M. (1994) Purification of T beta gamma subunit of transducin. *Methods Enzymol. 237*, 449–451.
37. Rubio, I., Pusch, R., and Wetzker, R. (2004) Quantification of absolute Ras-GDP/GTP levels by HPLC separation of Ras-bound [(32)P]-labelled nucleotides. *J. Biochem. Biophys. Methods 58*, 111–117.
38. Oprian, D. D., Molday, R. S., Kaufman, R. J., and Khorana, H. G. (1987) Expression of a synthetic bovine rhodopsin gene in monkey kidney cells. *Proc. Natl. Acad. Sci. U.S.A. 84*, 8874–8878.

39. Jastrzebska, B., Fotiadis, D., Jang, G. F., Stenkamp, R. E., Engel, A., and Palczewski, K. (2006) Functional and structural characterization of rhodopsin oligomers. *J. Biol. Chem. 281*, 11917–11922.
40. Fahmy, K., and Sakmar, T. P. (1993) Regulation of the rhodopsin-transducin interaction by a highly conserved carboxylic acid group. *Biochemistry 32*, 7229–7236.
41. Farrens, D. L., Altenbach, C., Yang, K., Hubbell, W. L., and Khorana, H. G. (1996) Requirement of rigid-body motion of transmembrane helices for light activation of rhodopsin. *Science 274*, 768–770.
42. Heck, M., and Hofmann, K. P. (2001) Maximal rate and nucleotide dependence of rhodopsin-catalyzed transducin activation: initial rate analysis based on a double displacement mechanism. *J. Biol. Chem. 276*, 10000–10009.
43. Baehr, W., Devlin, M. J., and Applebury, M. L. (1979) Isolation and characterization of cGMP phosphodiesterase from bovine rod outer segments. *J. Biol. Chem. 254*, 11669–11677.
44. Baehr, W., Morita, E. A., Swanson, R. J., and Applebury, M. L. (1982) Characterization of bovine rod outer segment G-protein. *J. Biol. Chem. 257*, 6452–6460.
45. Clack, J. W., Springmeyer, M. L., Clark, C. R., and Witzmann, F. A. (2006) Transducin subunit stoichiometry and cellular distribution in rod outer segments. *Cell Biol. Int. 30*, 829–835.
46. Artemyev, N. O., Arshavsky, V. Y., and Cote, R. H. (1998) Photoreceptor phosphodiesterase: interaction of inhibitory gamma subunit and cyclic GMP with specific binding sites on catalytic subunits. *Methods 14*, 93–104.
47. Oldham, W. M., Van Eps, N., Preininger, A. M., Hubbell, W. L., and Hamm, H. E. (2007) Mapping allosteric connections from the receptor to the nucleotide-binding pocket of heterotrimeric G proteins. *Proc. Natl. Acad. Sci. U.S.A. 104*, 7927–7932.
48. Oldham, W. M., and Hamm, H. E. (2008) Heterotrimeric G protein activation by G-protein-coupled receptors. *Nat. Rev. Mol. Cell. Biol. 9*, 60–71.
49. Fung, B. K., Hurley, J. B., and Stryer, L. (1981) Flow of information in the light-triggered cyclic nucleotide cascade of vision. *Proc. Natl. Acad. Sci. U.S.A. 78*, 152–156.
50. Skiba, N. P., Thomas, T. O., and Hamm, H. E. (2000) G alpha t/G alpha i1 chimeras used to define structural basis of specific functions of G alpha t. *Methods Enzymol. 315*, 502–524.
51. Skiba, N. P., Yang, C. S., Huang, T., Bae, H., and Hamm, H. E. (1999) The α-helical domain of Galphat determines specific interaction with regulator of G protein signaling 9. *J. Biol. Chem. 274*, 8770–8778.
52. Slepak, V. Z., Artemyev, N. O., Zhu, Y., Dumke, C. L., Sabacan, L., Sondek, J., Hamm, H. E., Bownds, M. D., and Arshavsky, V. Y. (1995) An effector site that stimulates G-protein GTPase in photoreceptors. *J. Biol. Chem. 270*, 14319–14324.
53. Abdulaev, N. G., Ngo, T., Ramon, E., Brabazon, D. M., Marino, J. P., and Ridge, K. D. (2006) The receptor-bound "empty pocket" state of the heterotrimeric G-protein alpha-subunit is conformationally dynamic. *Biochemistry 45*, 12986–12997.
54. Ridge, K. D., Marino, J. P., Ngo, T., Ramon, E., Brabazon, D. M., and Abdulaev, N. G. (2006) NMR analysis of rhodopsin-transducin interactions. *Vision Res. 46*, 4482–4492.
55. Ortiz, J. O., and Bubis, J. (2001) Effects of differential sulfhydryl group-specific labeling on the rhodopsin and guanine nucleotide binding activities of transducin. *Arch. Biochem. Biophys. 387*, 233–242.
56. Fung, B. K., and Nash, C. R. (1983) Characterization of transducin from bovine retinal rod outer segments. II. Evidence for distinct binding sites and conformational changes revealed by limited proteolysis with trypsin. *J. Biol. Chem. 258*, 10503–10510.
57. Hamm, H. E., Deretic, D., Arendt, A., Hargrave, P. A., Koenig, B., and Hofmann, K. P. (1988) Site of G protein binding to rhodopsin mapped with synthetic peptides from the alpha subunit. *Science 241*, 832–835.
58. Bartl, F., Ritter, E., and Hofmann, K. P. (2000) FTIR spectroscopy of complexes formed between metarhodopsin II and C-terminal peptides from the G-protein alpha- and gamma-subunits. *FEBS Lett. 473*, 259–264.
59. Kisselev, O. G., and Downs, M. A. (2003) Rhodopsin controls a conformational switch on the transducin gamma subunit. *Structure (Cambridge) 11*, 367–373.

BI8015444